

Short communication

## Improvement of solid oxide fuel cell performance by using non-uniform potential operation

S. Vivanpatarakij<sup>a</sup>, S. Assabumrungrat<sup>a,\*</sup>, N. Laosiripojana<sup>b</sup>

<sup>a</sup> Center of Excellence in Catalysis and Catalytic Reaction Engineering, Department of Chemical Engineering, Faculty of Engineering, Chulalongkorn University, Bangkok 10330, Thailand

<sup>b</sup> The Joint Graduate School of Energy and Environment, King Mongkut's University of Technology Thonburi, Bangkok 10140, Thailand

Received 7 November 2006; received in revised form 6 February 2007; accepted 6 February 2007

Available online 21 February 2007

### Abstract

Theoretical study was carried out to investigate the possible improvement of SOFC performance by using a non-uniform potential operation (SOFC-NUP) in which the operating voltage was allowed to vary along the cell length. Preliminary results of a simple SOFC-NUP with a cell divided into two sections of equal size in term of range of fuel utilization ( $U_f$ ) indicated that the SOFC-NUP can offer higher power density than an SOFC with uniform potential operation (SOFC-UP) without a reduction of the electrical efficiency. In this work, voltages and section splits were optimized to obtain the maximum power density of the SOFC-NUP. At the optimum splits ( $S_{p,1}=0.55$  and  $S_{p,2}=0.45$ ), the power density improvement as high as 9.2% could be achieved depending on the level of electrical efficiency. It was further demonstrated that the increase in the number of separated section ( $n$ ) of the cell could increase the achieved maximum power density but the improvement became less pronounced after  $n > 3$ .

© 2007 Elsevier B.V. All rights reserved.

**Keywords:** SOFC; Non-uniform potential; Power generation

### 1. Introduction

Fuel cells are promising electrochemical devices that convert the chemical energy of a fuel directly into electrical energy. Compared to conventional power generation processes, fuel cells are attractive due to their better environmental friendliness, practical noise-free operation, and higher efficiency. A number of researches have been carried out in many directions with a major aim to improve performances of the fuel cells and their systems. For instance, several gas turbine cycles such as steam injected gas turbine cycle, gas turbine/steam turbine combined cycle, and humid air turbine cycle have been combined with solid oxide fuel cell (SOFC) for efficiency improvement [1]. An operation with anodic offgas recirculation was proposed for a polymer electrolyte membrane fuel cell (PEMFC) system equipped with a fuel processor. Under this operation, a significant efficiency increase for the fuel processor and the gross

efficiency of the combined system of 30% were reported [2]. A novel gas distributor with current-collecting elements distributed in gas-delivery fields for effective current collection and heat/mass transfer enhancement was designed to improve power density [3,4]. In addition, many researches have been devoted on development of cell components with superior characteristics [5–7]. The performance improvement of PEMFC from operation at a higher pressure was reported although the power loss due to air compression was taken into account in the comparisons [8].

Among several procedures for improving fuel cell performance, the use of non-uniform potential operation concept for fuel cells in which the cell voltage is allowed to vary along the cell length is another interesting approach. However, until now only some works have focused on the potential benefits of this approach. It was demonstrated that an improvement in electrical efficiency of about 1% could be achieved by splitting the cell of a molten carbonate fuel cell (MCFC) into two sections [9]. Selimovic and Plasson [10] examined performances of networked solid oxide fuel cell (SOFC) stacks combined with a gas turbine cycle. Two multistage configurations, i.e. (i) both anode and cathode flows were serially connected and (ii) only the anode

\* Corresponding author. Tel.: +66 2 216 6868; fax: +66 2 218 6877.  
E-mail address: [Suttichai.A@chula.ac.th](mailto:Suttichai.A@chula.ac.th) (S. Assabumrungrat).

### Nomenclature

$a$	constant in Eq. (11) ( $\Omega$ m)
$A$	area ( $\text{m}^2$ )
$b$	constant in Eq. (11) (K)
$E$	activation polarization energy in Eqs. (12) and (13) ( $\text{kJ mol}^{-1}$ )
$E_0$	open circuit voltage (V)
$F$	Faraday constant (96485.34) ( $\text{C mol}^{-1}$ )
$i$	current density ( $\text{A m}^{-2}$ )
LHV	lower heating value of methane feed (W)
$m$	constant polarization parameters in Eqs. (12) and (13)
$n$	number of separated section
$p$	partial pressure (atm)
$P$	power density ( $\text{W cm}^{-2}$ )
$r$	activation polarization parameters in Eqs. (12) and (13) ( $\text{A m}^{-2}$ )
$R$	universal gas constant ( $8.31447 \times 10^{-3}$ ) ( $\text{kJ mol}^{-1} \text{K}^{-1}$ )
$S_p$	section split
$T$	absolute temperature (K)
$U_f$	fuel utilization (%)
$V$	operating voltage (V)
$W$	electrical work (W)

### Greeks letters

$\delta$	thickness (m)
$\varepsilon$	electrical efficiency (%)
$\eta$	overpotential ( $\Omega \text{m}^2$ )
$\varphi$	potential (V)
$\rho$	specific ohmic resistance ( $\Omega \text{m}$ )

### Subscript

A	anode
Act	activation
C	cathode
Conc	concentration
$k$	section number
Ohm	ohmic

flow was serially connected while the cathode flow was parallel connected, were considered. An increase of system efficiency of about 5% was reported for the former configuration mainly due to an improved thermal management. The similar multi-stage configurations were also considered for a combined heat and power MCFC plant [11]. Detailed flowsheet calculations showed that the improvement in efficiency was about 0.6% for the former configuration, and 0.8% for the latter configuration. The concept was also extended to PEMFCs divided into many stages (or stacks) of equal size [12]. It was demonstrated that the non-uniform cell potential operation allowed for enhanced maximum power densities compared to the traditional concept involving a uniform cell potential distribution. The improvement within 6.5% was reported.

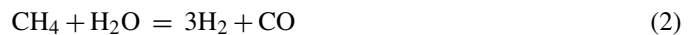
In this study, the concept of non-uniform potential operation implemented to SOFCs fed by methane was investigated in an effort to optimize cell operating voltages and sizes so that a maximum power density could be achieved without a reduction of electrical efficiency. Values of power density of a simple SOFC with a cell divided into two sections whose operating voltages and sizes were allowed to vary were compared to those of a typical SOFC with uniform cell potential at various electrical efficiencies. Additionally, the effect of number of cell section on the obtained performance was determined.

## 2. Theory

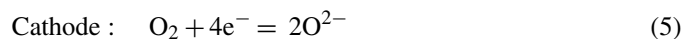
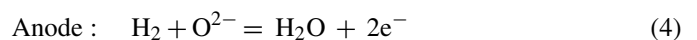
The schematic diagram of an SOFC with non-uniform potential operation (SOFC-NUP) is illustrated in Fig. 1. Compositions of fuel and air streams change along the cell channel according to changes in value of fuel utilization defined as the mole of hydrogen electrochemically consumed divided by the theoretical mole of hydrogen generated from complete reforming of the methane feed. In section  $k$ , the fuel utilization changes from  $U_{f,k-1}$  to  $U_{f,k}$ , and the cell is operated at a constant potential of  $V_k$  within the section. In practice, the non-uniform cell potential can be realized by using segmented current collectors for a single-cell SOFC or it can be carried out in a series of SOFC stacks operated at different stack potentials. The section split of section  $k$  ( $S_{p,k}$ ) is defined by

$$S_{p,k} = \frac{U_{f,k} - U_{f,k-1}}{U_{f,\text{final}}} \quad (1)$$

When the SOFC is fed by a non-hydrogen fuel (e.g. methane), a reformer is generally required to reform the fuel with an oxidant (e.g. steam) to a hydrogen-rich stream before feeding to the SOFC stack. The main reactions involved in the production of hydrogen from methane and steam are the methane steam reforming and water gas shift reactions as shown in Eqs. (2) and (3), respectively.



In the SOFC stack, both hydrogen and CO can react electrochemically with oxygen. However, it is assumed that the CO electro-oxidation is neglected. It was estimated earlier that about 98% of current is produced by  $\text{H}_2$  oxidation in common situations [13]. This is due to the fast rate of water gas shift reaction at an SOFC operating temperature. The electrochemical reactions of hydrogen and oxygen take place according to Eqs. (4) and (5).



Electromotive force ( $E_0$ ) of the cell is a difference of potentials between both electrodes of the cell. It can be represented as follows:

$$E_0 = |\varphi_C - \varphi_A| \quad (6)$$

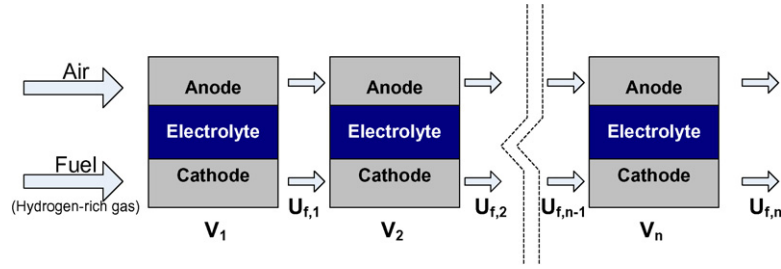


Fig. 1. Schematic diagrams of SOFC-NUP.

where  $\varphi_C$  and  $\varphi_A$  are the potentials of the cathode and the anode, respectively. The electrode potential can be calculated from Nernst equation which can be expressed as follows:

$$\varphi = \left( \frac{RT}{4F} \right) \ln p_{O_2} \quad (7)$$

where  $R$  is the universal gas constant,  $T$  the absolute temperature and  $F$  is the Faraday's constant. The partial pressure of oxygen in the cathode chamber is calculated from its mole fraction while the partial pressure of oxygen in the anode chamber is given by:

$$p_{O_2} = \left( \frac{p_{H_2O}}{K p_{H_2}} \right)^2 \quad (8)$$

where  $p_i$  is the partial pressure, and  $K$  is the equilibrium constant of the hydrogen oxidation reaction.

When the SOFC is operated at a potential of  $V_k$ , the local current density can be determined according to Eq. (9). It should be noted that as the value of  $E_0$  changes along the cell length within the section due to the change in gas compositions, the current density varies within the cell section.

$$i = \frac{E_0 - V_k}{\eta_{Ohm} + \eta_{Act,A} + \eta_{Act,C} + \eta_{Conc,A} + \eta_{Conc,C}} \quad (9)$$

where

$$\eta_{Ohm} = \sum \rho_j \delta_j \quad (10)$$

$$\rho_j = a_j \exp(b_j T) \quad (11)$$

$$\eta_{Act,C} = \left( \frac{4F}{RT} r_C \left( \frac{p_{O_2}}{p} \right)^m \exp \left( \frac{-E_C}{RT} \right) \right)^{-1} \quad (12)$$

$$\eta_{Act,A} = \left( \frac{2F}{RT} r_A \left( \frac{p_{H_2}}{p} \right)^m \exp \left( \frac{-E_A}{RT} \right) \right)^{-1} \quad (13)$$

The parameters used in the calculations are provided in Table 1 [14] and Table 2 [15]. It was reported that the correlations of the activation polarization can predict the cell performance close to the Butler–Volmer equation within the temperature range of 1173–1273 K [16]. In this study, the operating temperature is kept at 1173 K which is in the reliable limit.

To simplify the calculations of the SOFC performance, it is assumed that both fuel and oxidant are well-diffused through the surface of the electrodes. Therefore, concentration polarization losses ( $\eta_{Conc,A}$  and  $\eta_{Conc,C}$ ) can be omitted. This assumption

Table 1  
Resistivity and thickness of cell component [12]

Material used	Ni-YSZ/YSZ/LSM-YSZ
Anode thickness ( $\mu\text{m}$ )	150
Anode ohmic resistance constant	$a = 0.0000298, b = -1392$
Cathode thickness ( $\mu\text{m}$ )	2000
Cathode ohmic resistance constant	$a = 0.0000811, b = 600$
Electrolyte thickness ( $\mu\text{m}$ )	40
Electrolyte ohmic resistance constant	$a = 0.0000294, b = 10350$
Interconnect thickness ( $\mu\text{m}$ )	10
Interconnect ohmic resistance constant	$a = 0.001256, b = 4690$

is valid when the cell is not operated at too high current density or too low concentration. In addition, it is further assumed that the cell is operated at isothermal condition and the fuel stream is always at its equilibrium composition along the length of the SOFC cell. It should be noted that an external reformer is usually connected to the SOFC system in order to generate hydrogen-rich feed for the stack and to suppress the cell deactivation due to the carbon formation. In addition, state-of-the-art SOFC nickel cermet anodes are usually active for the steam reforming and shift reactions particularly at high operating temperature of SOFC [16,17]. Calculations of the thermodynamic equilibrium composition are accomplished by following details given in our previous work [18].

When the current density is known, the cell area ( $A_k$ ) and electrical power ( $W_k$ ) involved in each cell section can be determined. The values of overall electrical efficiency ( $\varepsilon$ ) and average power density ( $P$ ) can be determined according to Eqs. (14) and (15), respectively.

$$\varepsilon = \sum_{k=1}^n \frac{W_k}{\text{LHV}} \times 100\% \quad (14)$$

$$P = \frac{\sum_{k=1}^n W_k}{\sum_{k=1}^n A_k} \quad (15)$$

where LHV is the lower heating value of methane feed.

Table 2  
Summary of activation polarization parameters [13]

	$r$ ( $\text{A m}^{-2}$ )	$E_{A,\text{pol}}$ ( $\text{kJ mol}^{-1}$ )	$m$
Cathode	$1.489 \times 10^{10}$	160	0.25
Anode	$2.128 \times 10^8$	110	0.25

### 3. Results and discussion

Fig. 2 shows the performances of a typical SOFC with uniform potential operation (SOFC-UP). Each line represents the results at a constant value of fuel utilization ( $U_f$ ). It should be noted that because concentration polarization becomes an importance loss at high current densities and small fuel concentrations ( $U_f \geq 80\%$ ) [15], the simulations were performed only in the ranges of high voltages (low current densities) and fuel utilizations ( $U_f$ ) of lower than 80%. In order to validate the calculations, the simulation results from a previous literature [19] at a condition close to our work ( $U_f = 85\%$ ) are included in Fig. 2. Our calculations show good agreement within a range of high operating voltages (0.65–0.75 V). However, at lower voltages, the data from the literature shows higher power density. This is probably due to the observed temperature increase (within 100 K) which is particularly pronounced at high current density (low voltage) whereas our calculations were based on the isothermal condition. From Fig. 2, regarding the electrical efficiency, it is favorable to operate the SOFC at high voltage in order to obtain high efficiency. However, when taking into account the power density, operation at a high value of voltage is not practical due to the achievement of low power density. Therefore, in practice suitable operating voltage and fuel utilization should be carefully selected. Some workers suggested to operate the cell at 70% of maximum power density [20] and fuel utilization of 80–95% [21–24]. In the present work, the fuel utilization ( $U_f$ ) of 80% was considered and SOFC with non-uniform potential operation (SOFC-NUP) was investigated with the aim to improve the power density without lowering the electrical efficiency.

Fig. 3 shows the relationship between power density and electrical efficiency of a simple SOFC-NUP with a cell divided into two sections of equal range of fuel utilization ( $S_{p,1} = S_{p,2} = 0.5$ ).  $V_1$  and  $V_2$  represent the operating voltages of sections 1 and 2, respectively. The thick solid line indicates the results of the SOFC-UP. It is indicated that there are some ranges of operation in which the SOFC-NUP offers higher power density than the SOFC-UP without lowering the electrical efficiency (area above of the thick solid line). The improvement becomes significant when the cell is operated at high electrical efficiency.

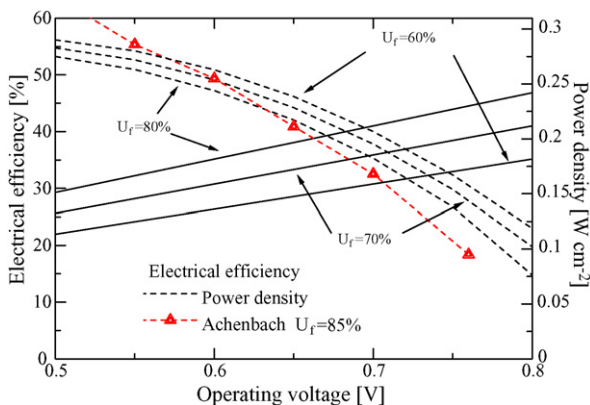


Fig. 2. Performance characteristic curves of typical SOFC-UP ( $H_2O/CH_4$  ratio = 2.2 and  $T = 1173$  K).

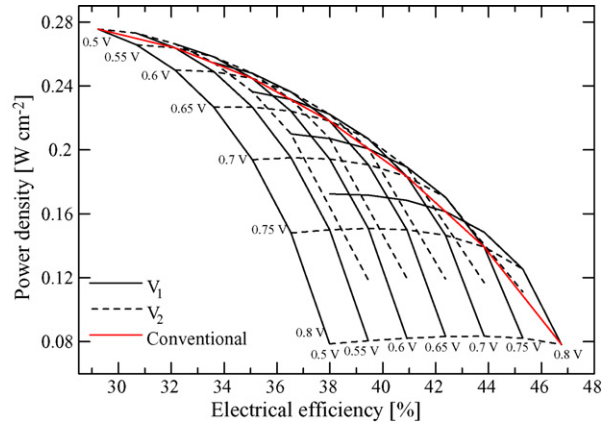


Fig. 3. Relationship between power density and electrical efficiency of SOFC-UP and SOFC-NUP ( $U_f = 80\%$  and  $T = 1173$  K; for SOFC-NUP:  $n = 2$ ,  $S_{p,1} = 0.5$ ).

In order to indicate suitable operating voltages which offer the highest average power density, the value of electrical efficiency was specified and the value of  $V_1$  was varied. Then  $V_2$ , which gives the desired value of the electrical efficiency, and its corresponding power density can be calculated. For example, as shown in Fig. 4, for an electrical efficiency of 43%, the values of  $V_2$  are 0.623, 0.673 and 0.723 V for  $V_1 = 0.7, 0.75$  and  $0.80$  V, respectively, and the corresponding values of the power density are 0.178, 0.156 and 0.159  $W\ cm^{-2}$ , respectively. By varying  $V_1$ , the maximum power density of 0.162  $W\ cm^{-2}$  is obtained at  $V_1 = 0.773$  V and  $V_2 = 0.700$  V.

According to the above study, the section splits were maintained at  $S_{p,1} = S_{p,2} = 0.5$ . Those values were then adjusted in order to achieve better performance. Fig. 5 shows the effect of section split ( $S_{p,1}$ ) on the power density improvement at different values of electrical efficiency. It should be noted that the reported values are based on the operation using optimum voltages for each value of the section split. It was found that the power density improvement as high as 9.2% can be achieved at the electrical efficiency of 45% but the improvement becomes less significant when the SOFC is operated at lower electrical efficiency. In addition, the optimum  $S_{p,1}$  for all cases was found

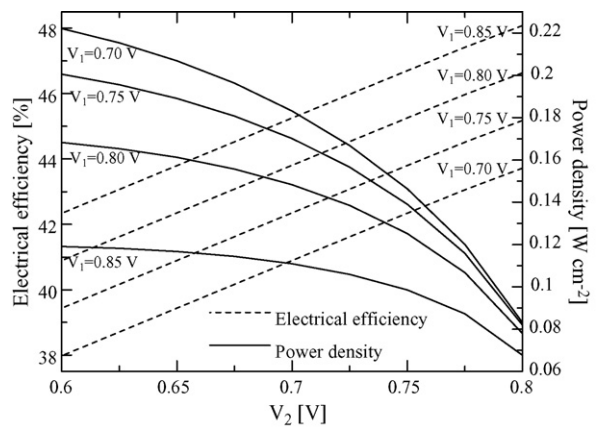
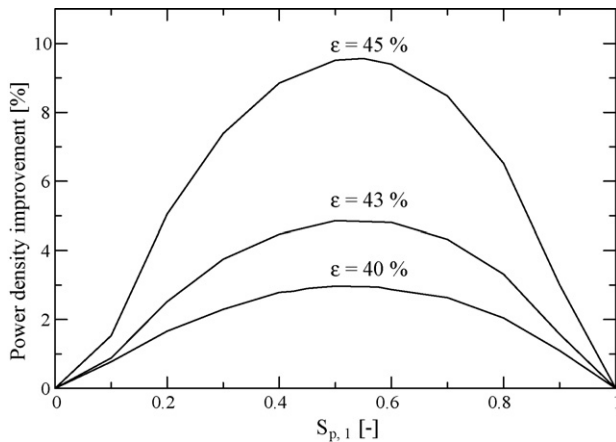


Fig. 4. Effect of operating voltages on performance of SOFC-NUP ( $n = 2$ ,  $U_f = 80\%$ ,  $T = 1173$  K,  $S_{p,1} = 0.5$  and  $S_{p,2} = 0.5$ ).

Table 3

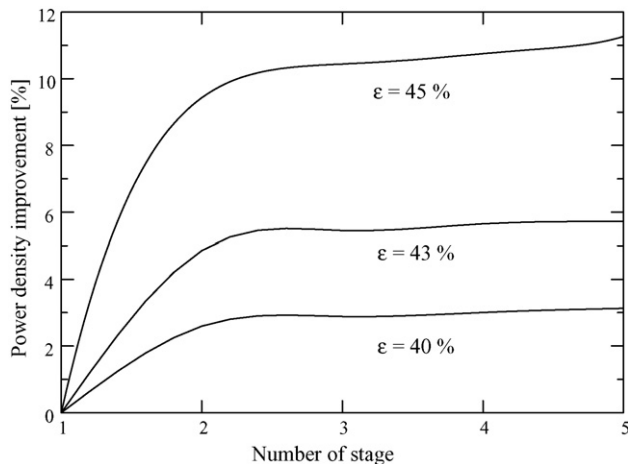
Comparison of power density between SOFCs with different number of section and section splits

Electrical efficiency (%)	Power density ( $\text{W cm}^{-2}$ )			
	$n = 1$	$n = 2$ ( $S_{p,1} = S_{p,2} = 0.5$ )	$n = 2$ ( $S_{p,1} = 0.55, S_{p,2} = 0.45$ )	$n = 3$ ( $S_{p,1} = S_{p,2} = S_{p,3} = (1/3)$ )
35	0.246 (0.598 V)	0.248 (0.619, 0.571 V)	0.249 (0.631, 0.560 V)	0.250 (0.644, 0.608, 0.544 V)
37	0.229 (0.632 V)	0.232 (0.669, 0.598 V)	0.232 (0.666, 0.594 V)	0.233 (0.682, 0.632, 0.583 V)
40	0.196 (0.683 V)	0.201 (0.721, 0.649 V)	0.201 (0.717, 0.645 V)	0.202 (0.740, 0.666, 0.647 V)
43	0.154 (0.734 V)	0.162 (0.7726, 0.7001 V)	0.162 (0.768, 0.697 V)	0.164 (0.782, 0.736, 0.688 V)
45	0.120 (0.768 V)	0.131 (0.8069, 0.7342 V)	0.131 (0.803, 0.731 V)	0.134 (0.817, 0.772, 0.720 V)

Fig. 5. Effect of section split on power density improvement of SOFC-NUP ( $n = 2$ ,  $U_f = 80\%$  and  $T = 1173 \text{ K}$ ).

to be around 0.55. Table 3 summarizes the values of the power density and the corresponding optimum voltages at different electrical efficiency of the SOFC-UP and the SOFC-NUPs with  $S_{p,1} = S_{p,2}$  and with the optimum  $S_{p,1}$  and  $S_{p,2}$ . It was found that the results of the SOFC-NUP with the optimum  $S_{p,1}$  and  $S_{p,2}$  are not significantly different from those of the SOFC-NUP with  $S_{p,1} = S_{p,2}$  although the voltages are different.

To further enhance the performance of the SOFC-NUP, the number of separated section ( $n$ ) was increased. Fig. 6 shows the effect of the number of section on the power density improve-

Fig. 6. Effect of number of stage on power density improvement of SOFC-NUP ( $U_f = 80\%$ ,  $T = 1173 \text{ K}$  and  $S_{p,k} = 1/n$ ).

ment for three values of electrical efficiency. The section splits of all sections are specified to be at the same value of  $S_{p,k} = 1/n$  in order to simplify the calculations. The optimum voltages of the SOFC-NUPs which offer the highest power density for each case were determined by following the procedure described earlier for the case with  $n = 2$ . It was assumed that the maximum power density achieved from the case with adjustable section splits does not significantly differ from that achieved from the case with equally divided sections. This assumption is valid at least for the case of the SOFC-NUP with  $n = 2$  as shown earlier. The calculated results indicate that the obtained maximum power density increases with increasing the number of sections ( $n$ ). However, the improvement becomes less significant after  $n > 3$ . The SOFC-NUP with  $n = 3$  is likely to be a suitable system for improving the power density without the reduction of electrical efficiency. Table 3 also shows the values of the maximum power density and the corresponding voltages at different values of electrical efficiency. At the electrical efficiency of 45%, the power density of the SOFC-NUP with  $n = 3$  is 11.7% higher than that of the typical SOFC-UP.

From the above results, it has been demonstrated that the use of the non-uniform potential operation with SOFC is technically feasible. The cell area can be reduced without lowering the electrical efficiency. However, the SOFC-NUP would require more sophisticated cell arrangement, power conditioning system and so on. The system control would inevitably become more complicated. Further investigations are required before implementing this system for commercial use.

#### 4. Conclusions

An SOFC-NUP can provide higher power density than a typical SOFC-UP without a reduction of electrical efficiency. The optimum SOFC-NUP was determined by allowing the operating voltage and section split of each section to be appropriately adjusted to achieve the highest power density for each level of electrical efficiency. The maximum power density can be further improved by increasing the number of separated section ( $n$ ) of the cell; however, it became less pronounced after  $n > 3$ . Although it is obvious that the non-uniform operation can allow the SOFC to be operated at higher performance, further investigation is necessary to determine whether the cost reduction by the reduced stack size would be sufficiently attractive compared to the increases of power conditioning cost and complication of the SOFC operation.

## Acknowledgements

The supports from The Thailand Research Fund and Commission on Higher Education are gratefully acknowledged. The second author also would like to acknowledge kind supports from Professor Piyasan Prasertthdam.

## References

- [1] P. Kuchonthara, S. Bhattacharya, A. Tsutsumi, *J. Power Sources* 124 (2003) 65–75.
- [2] A. Heinzl, J. Roes, H. Brandt, *J. Power Sources* 145 (2005) 312–318.
- [3] P.W. Li, S.P. Chen, M.K. Chyu, *J. Power Sources* 140 (2005) 311–318.
- [4] Y.G. Yoon, W.Y. Lee, G.G. Park, T.H. Yang, C.S. Kim, *Electrochim. Acta* 50 (2004) 709–712.
- [5] S.P. Yoon, J. Han, S.W. Nam, T.H. Lim, S.A. Hong, *J. Power Sources* 136 (2004) 30–36.
- [6] S.D. Kim, S.H. Hyun, J. Moon, J.H. Kim, R.H. Song, *J. Power Sources* 139 (2005) 67–72.
- [7] S.P. Simner, J.F. Bonnett, N.L. Canfield, K.D. Meinhardt, J.P. Shelton, V.L. Sprenkle, J.W. Stevenson, *J. Power Sources* 113 (2003) 1–10.
- [8] A. Kazim, *J. Power Sources* 143 (2005) 9–16.
- [9] F. Standeart, Analytical fuel cell modelling and exergy analysis of fuel cells, Ph.D. Thesis, Delft University of Technology, 1998.
- [10] A. Selimovic, J. Palsson, *J. Power Sources* 106 (2002) 76–82.
- [11] S.F. Au, N. Woudstra, K. Hemmes, *J. Power Sources* 122 (2003) 28–36.
- [12] S.M. Senn, D. Poulidakos, *Electrochem. Commun.* 7 (2005) 773–780.
- [13] M.A. Khaleel, Z. Lin, P. Singh, W. Surdoval, D. Collin, *J. Power Sources* 130 (2004) 136–148.
- [14] S.H. Chan, C.F. Low, O.L. Ding, *J. Power Source* 103 (2002) 188–200.
- [15] E. Hernandez-Pacheco, D. Singh, P.N. Hutton, N. Patel, M.D. Mann, *J. Power Sources* 138 (2004) 174–186.
- [16] S.H. Clarke, A.L. Dicks, K. Pointon, T.A. Smith, A. Swann, *Catal. Today* 38 (1997) 411–423.
- [17] A.L. Dicks, *J. Power Sources* 71 (1998) 111–122.
- [18] W. Sangtongkitcharoen, S. Assabumrungrat, V. Pavarajarn, N. Laosiripojana, P. Prasertthdam, *J. Power Source* 142 (2005) 75–80.
- [19] E. Achenbach, *J. Power Sources* 49 (1994) 333–348.
- [20] A.K. Demin, P. Tsiakaras, E. Gorbova, S. Hramova, *J. Power Sources* 131 (2004) 231–236.
- [21] J.R. Rostrup-Nielsen, *Phys. Chem. Chem. Phys.* 3 (2001) 283–288.
- [22] S. Campanari, *J. Power Sources* 92 (2001) 26–34.
- [23] E. Riensche, U. Stimming, G. Unverzagt, *J. Power Sources* 73 (1998) 251–256.
- [24] A. Criscuoli, A. Basile, E. Drioli, O. Loiacono, *J. Membr. Sci.* 181 (2001) 21–27.